Gabriele Colaoni

COMPOSITE MATERIALS *for* TECHNICAL EDUCATION

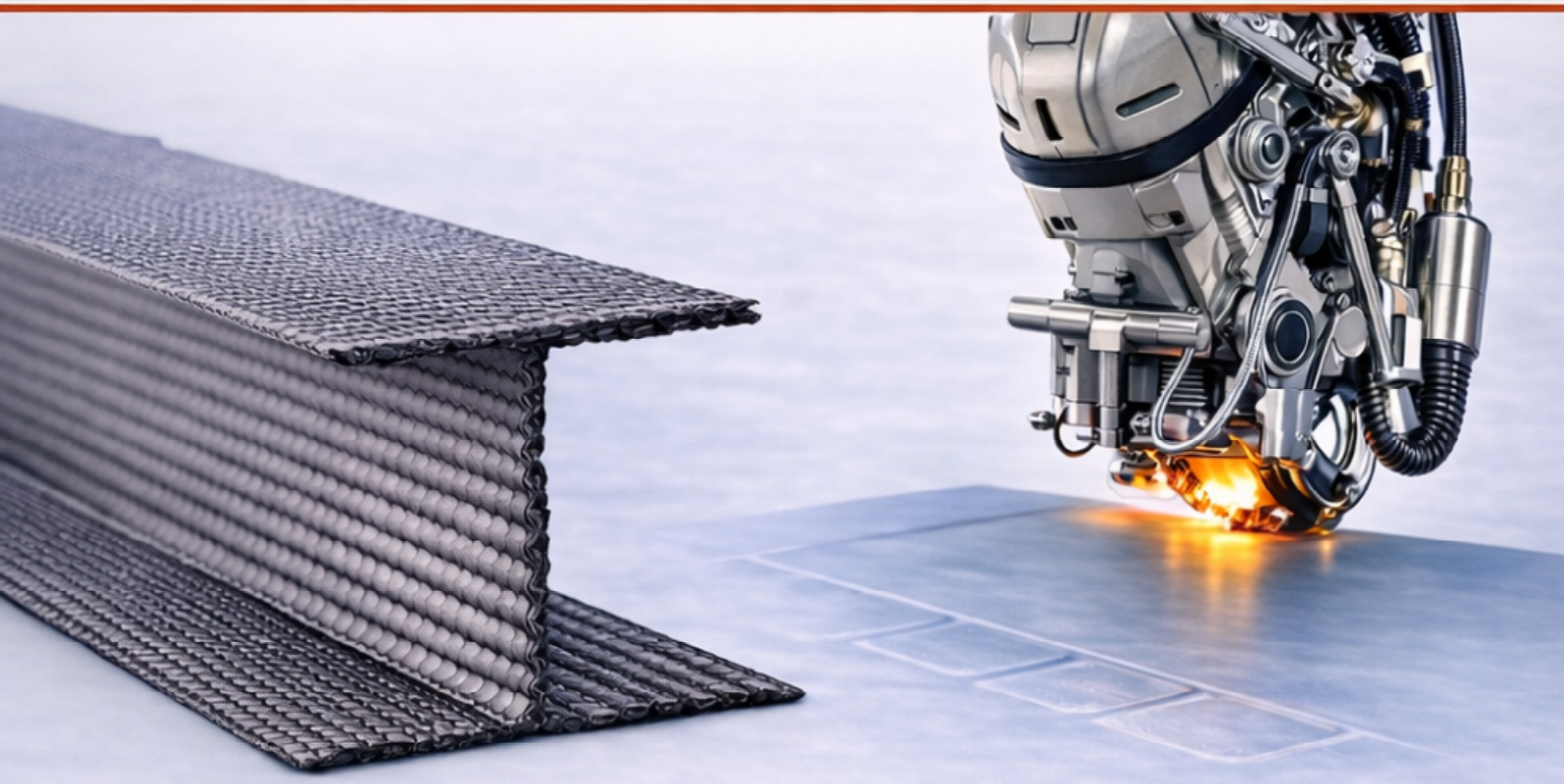

Process · Theory · Properties

2nd edition | 2026

Inside QR-linked contents!

For students, engineers and R&D teams

Gabriele Colaoni

Composite Materials for Technical Education

Process - Theory – Properties

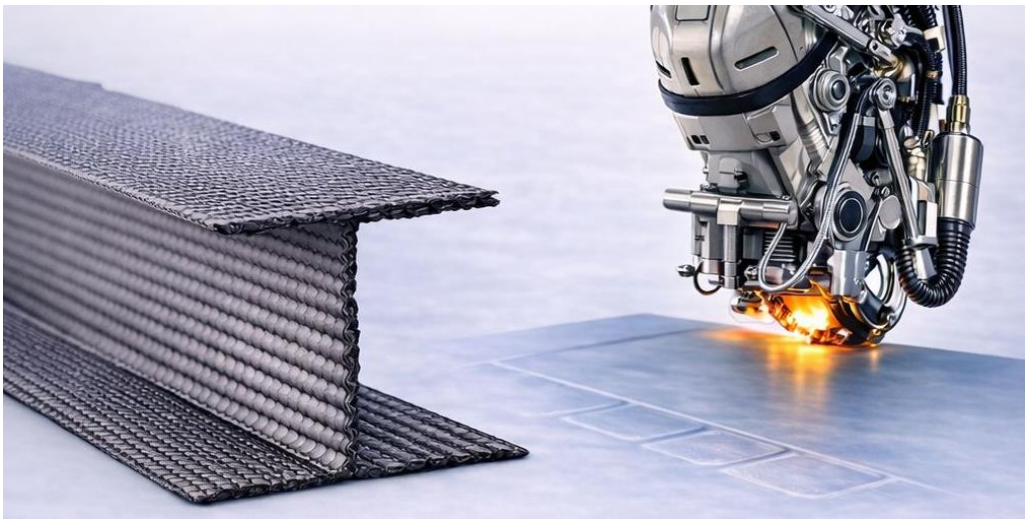

Zurich, 2026 – 2nd edition

About this book

Composite materials are now part of everyday industrial reality, from lightweight structures to high-performance products, yet they are still often taught in fragments, without a clear bridge to the workshop and the factory floor.

Composite Materials for Technical Education (Process- Theory- Properties) was written to provide that bridge, offering a structured, practical path that connects fundamentals to real manufacturing and engineering decisions.

- **Who it is for:**

  technical students, early-career technicians, and anyone who needs a clear, practical introduction to composites without oversimplification.

- **Also ideal for:**

  teachers and technical trainers who want a reliable backbone for lessons, exercises, and lab activities.

- **Useful in industry onboarding:**

  for new hires in production, quality, and industrialization who must quickly learn correct terminology, typical issues, and best practices.

- **For companies transitioning into composites:**

  especially teams coming from metal-mechanical backgrounds who need solid fundamentals and a process-oriented mindset.

- **Role in technical education:**

  to bridge theory and real manufacturing (linking material behavior, processing methods, defects, and design choices to cost, safety, and producibility) so learners can operate confidently in both workshop and engineering environments.

What you will learn

In this book you will learn how to:

- understand composite materials through the **process–structure–property relationship**, rather than as isolated topics
- recognize the **main manufacturing routes** for composites and their implications on quality, cost, and performance
- read composite behaviour from a **load-driven perspective**, tracing forces before choosing materials or lay-ups
- identify **typical manufacturing defects and process limits**, and understand how they originate
- move confidently between **workshop practice and engineering reasoning,** using correct terminology and sound fundamentals
- develop a **process-oriented mindset** suitable for production, industrialization, and early design decisions

Throughout the book, **QR codes provide direct access to selected external resources** for deeper exploration, including authoritative technical references and applied examples.

Readers also have access to an **up-to-date materials database**, intended to support comparisons, property evaluation, and informed material selection alongside the concepts discussed in the text.

About the Author

Gabriele Colaoni sees engineering as the art of **making strength look effortless**.

For more than twenty years he has pursued that ideal across the most demanding arenas of lightweight design, from the split-second world of top-tier motorsport to the silent precision of autonomous flight and the wave-piercing agility of foiling craft.

He first cut his teeth on carbon-fibre components that had to survive hundreds of kilometres at full throttle on racing tracks while adding almost no mass to the car. The same quest for gram-level efficiency later carried him into pioneering aerospace programmes, where electric vertical-lift aircraft and long-endurance drones trade every saved ounce for extra minutes of range.

Water soon joined asphalt and sky.

High-speed foiling hulls and modular deck panels made the open water his toughest tutor. They showed him that when fibres run with the water-borne loads the structure stops behaving like a brittle shell and starts working like a resilient spring. The takeaway was lasting: map the forces first, let the lay-up follow, and the sea will pay you back with speed and reliability.

Advanced industrial tooling later entered his portfolio, each new field reaffirming a simple lesson: materials may change, but **the discipline of tracing forces and letting the laminate do the work is universal.**

Today Gabriele balances design programs with mentoring and technical writing. His goal is always the same: **turn insider know-how into clear narratives that others can apply.**

Composite Materials for Technical Education embodies that ambition, offering readers not just formulas and diagrams but the mindset behind them: look for the critical load, respect the material, and let lightness do the talking.

In spare moments he sketches future airframes and follows emerging trends in sustainable composites, convinced that **the most elegant solution is usually the one you almost don’t notice because it is exactly where it needs to be, and no heavier than absolutely necessary.**

Evolution and application of composites

Composite materials represent a hybrid class of engineering materials, positioned between polymers, metals, and ceramics. A composite is defined as the intentional combination of two distinct phases: a matrix, typically present in greater volume, and a reinforcement, which enhances overall mechanical performance. Each phase retains its inherent chemical and physical characteristics within the composite, resulting in a synergistic material system.

Adhesion between the matrix and reinforcement is often improved through the application of a *sizing agent*, generally a nanoscale surface coating on the reinforcement that promotes chemical compatibility. While this interphase does not directly contribute to the bulk mechanical properties, it plays a crucial role in long-term durability and in the efficient transfer of loads between matrix and reinforcement.

Beyond the primary reinforcement, matrices may incorporate fillers, such as talc, silica, calcium carbonate, rubber particles, or carbon nanotubes, aimed at modifying properties not effectively controlled by the main reinforcement. These additives can improve toughness, reduce shrinkage during molding, or increase electrical conductivity, and their use has become routine in industrial formulations.

It's important to distinguish *structural composites* from *micro-* or *nanocomposites* formed by homogeneous dispersion or precipitation (e.g., metallic alloys, doped polymers, or particle-filled plastics). True composites are macroscopically multiphasic, with a *distinct morphology and scale separation between phases.*

A significant innovation in composite technology has been the introduction of reinforcements with high aspect ratios (i.e., long fibers or tapes), necessitating alternative manufacturing methods beyond those traditionally used for polymers or metals. These include filament winding, pultrusion, lamination, and vacuum-assisted forming techniques. More recently, additive manufacturing approaches have emerged, particularly for rapid prototyping and custom geometries. The choice of processing method is deeply influenced by the matrix type, which divides composite manufacturing into three major families: polymer matrix composites (PMCs), metal matrix composites (MMCs), and ceramic matrix composites (CMCs).

MMCs are fabricated using processes like powder metallurgy, diffusion bonding, or hot pressing. Due to their high production costs, their use is generally limited to high-temperature structural applications, where conventional metal alloys (including those based on titanium, beryllium, or nickel) fall short. MMCs often compete with CMCs, which offer better thermal stability and specific stiffness in similar conditions.

CMCs, with matrices composed of alumina, carbides, or silicates, combine ceramic toughness and thermal resistance. Although their market penetration is still modest, it's expected to grow significantly due to increasing demand in aerospace, hypersonic vehicles, and energy systems that require high-temperature operation without catastrophic brittle failure.

PMCs represent the most widespread class. They range from widely used glass-fiber-reinforced polymers (GFRP) to high-performance carbon-fiber-reinforced polymers (CFRP) and specialty systems using epoxy, phenolic, or polyimide matrices. The initial development of PMCs focused on embedding continuous fibers into thermoplastic matrices, improving strength-to-weight ratios and processability.

However, due to the high viscosity and poor flow of many thermoplastics, thermosetting resins such as epoxies became dominant. These resins, initially liquid, exhibit excellent wetting characteristics and ease of impregnation but require careful control of curing and cross-linking chemistry.

Recent advances have rekindled interest in high-performance thermoplastics, notably *polyaryletherketones* (PAEK, PEEK), which outperform epoxies in mechanical properties and chemical resistance. Their processing, however, requires elevated temperatures to achieve matrix flow, adding complexity and cost. In response, solid-state impregnation methods, like co-weaving or commingling of matrix and reinforcement fibers, have been introduced, allowing for simplified forming via a single thermal cycle, reducing energy costs and increasing manufacturing efficiency.

Within the PMC, MMC, and CMC domains, a subclass known as *advanced composites* has emerged. These typically feature continuous fiber reinforcement at high volume fractions, with stringent quality controls and superior performance. Although PMCs remain dominant due to their ease of processing and lightweight nature, there's growing industrial effort to develop affordable advanced CMCs and MMCs for extreme environments. *Advanced composites* are primarily used in structural applications subjected to extreme mechanical or thermal loads and requiring a high strength-to-weight ratio and environmental resistance. These materials originated in aerospace and defense and demand specialized design and processing capabilities.

The first significant wave of *structural composite* use occurred during the 1950s–60s aerospace boom, driven by performance demands and supported by government-funded R&D. Since then, composite applications have diversified into

marine, automotive, civil construction, energy, and sporting goods, making the sector one of the fastest-growing in materials engineering, second only to digital technologies.

A landmark in aerospace composite application is the Boeing 787 Dreamliner, introduced in 2011. This aircraft was the first commercial airliner to feature a fuselage and wings made primarily of carbon fiber-reinforced plastic (CFRP), with composites accounting for approximately 50% of the aircraft's weight and 80% of its volume. The extensive use of composites contributed to a 20% improvement in fuel efficiency compared to previous-generation aircraft, along with enhanced passenger comfort due to higher cabin humidity and lower cabin altitude pressurization.

→ For a deeper look at how composite materials evolved within major aerospace programs, this NASA report offers valuable historical context and technical insights. Scan this QR code:

In motorsport, particularly Formula One, composites have been used extensively for chassis, bodywork, and aerodynamic elements. The introduction of carbon fiber

composite materials to the chassis revolutionized car design, making them significantly lighter, stronger, and more rigid. This game-changing development transformed the way teams approached car design and allowed them to push the limits of performance.

Looking ahead, the automotive industry is poised to become the most dynamic sector for composite development. The need to reduce vehicle weight, enhance energy efficiency, and meet environmental regulations is fostering the adoption of composite components not only for structural parts but also for energy storage integration. Notably, Volvo's research into embedding batteries within CFRP body panels highlights a radical shift in multifunctional material design.

Despite their many advantages, composites face a significant challenge: end-of-life management and sustainability. While they often outperform traditional materials in lifecycle impact during in-use phases, the production emissions and lack of cost-effective recycling technologies remain major obstacles. Addressing these limitations is critical to ensuring the future viability of composites in a circular economy.

Contents

Part one
Technological processes for composites

Process-structure-property interdependence

The processing of composite materials is intrinsically linked to the transformations undergone by the matrix.

For thermoplastics, these involve physical state changes, while for thermosets, chemical-physical transitions define the so-called "processability window," ultimately determining the final properties of the material.

Fibers serve as the primary load-bearing elements due to their high strength and elastic modulus. Their orientation, as elucidated in *Lamination Theory*, must align with the intended application of the composite. This orientation is heavily influenced by the chosen manufacturing technology. For instance, in filament winding (a process extensively utilized in aerospace applications such as rocket motor casings) the necessity to maintain fiber tension mandates rapid curing mechanisms, achievable only with specialized resin formulations.

The interdependence of process, structure, and properties necessitates a holistic design approach. In composite engineering, it's imperative to consider available technologies, market-ready resins, and appropriate processing conditions to achieve the desired structural attributes. Often, the synergy of resin types, processing variables, and geometries constitutes proprietary knowledge within companies, colloquially termed as a "recipe," derived from extensive experimentation and iterative development.

The multitude of factors influencing material quality and performance allows for similar products to be manufactured using diverse technologies. Conversely, a single technology can yield varied products. For example, the production of

marine hulls employs techniques ranging from manual lamination to vacuum infusion and resin transfer molding. Conversely, autoclave processing, a staple in aerospace manufacturing, facilitates the creation of components ranging from intricate parts to large load-bearing structures. Economic considerations and certification requirements often dictate the association of specific products with defined processes, especially in high-tech sectors where substantial R&D investments necessitate long-term amortization.

Over the past six decades, composite production methodologies have evolved through a process of "scaling," leading to the development of dimensionless parameters characteristic of each process. These descriptors, independent of scale, aid in modeling the complex interplay between process, structure, and properties. Given the anisotropic nature of composites, viscoelastic behavior of matrices, and material heterogeneity, such modeling is intricate and typically requires computational tools, always necessitating experimental validation.

Micromechanical modeling, focusing on small material segments where phases and interphases are distinctly identified, is prevalent in academic research. Tools like MIT's Object-Oriented Finite element (OOF) software facilitate the understanding of various physical and chemical parameters within composites and their processing. However, these models often lack immediate applicability in industrial process definitions.

In contrast, *macromechanical* finite element modeling treats composites as equivalent orthotropic homogeneous solids or as shells with localized laminate properties. In these models, laminate properties are considered outcomes of the process,

generally defined experimentally after establishing all variables.

Currently, computational limitations restrict the integration of micro- and macrostructural modeling, confining them to academic research and industrial applications, respectively. The aerospace industry has historically spearheaded the development of advanced numerical solutions and processes. The stringent demands for specific performance metrics (structural integrity, thermal resilience, and reliability coupled with mass reduction) have led to the adoption of comprehensive computational tools for composites. Over time, the industry's need for standardization and certification has consolidated these methodologies into a few robust codes, such as NASTRAN, originally developed in the 1970s and still in use today.

Outside the aerospace sector, in environments with less stringent certification requirements, more user-friendly software solutions have emerged. These include plug-ins for multiphysics applications that seamlessly integrate with Computer-Aided Design (CAD) tools, such as the Advanced Composites Prepost (ACP) module in ANSYS or composite-specific functionalities within CATIA's Generative Part Structural Analysis (GPS) module.

Figure 1 - Industrial autoclave during loading, with a composite component already vacuum-bagged on its tooling and prepared for the curing cycle.

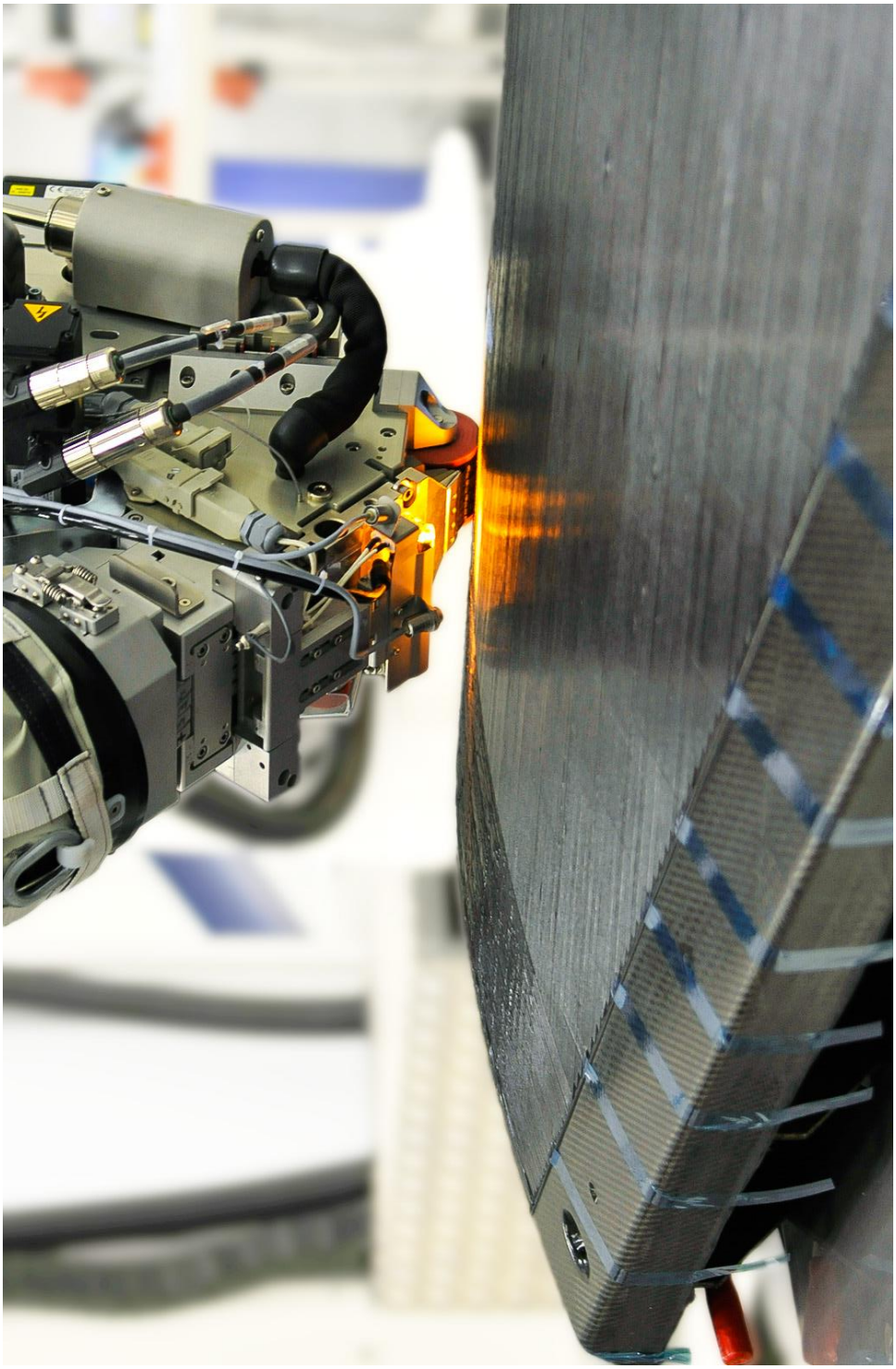

Figure 2 - Automated fiber placement (AFP) head depositing carbon fiber tows onto a contoured aerospace tool, with localized heating ensuring proper consolidation during layup.

Clearly, solubility is favored in purely energetic terms if polymer and solvent have similar solubility parameters that can be evaluated by simple experimental tests.

→ This QR gives a practical, calculation-oriented method to estimate solubility parameters via group contributions (Fedors approach).

Models for thermosetting resins

At sufficiently high temperatures, the polymerization (cross-linking) process begins with the formation of an infusible, insoluble three-dimensional network that is essentially a copolymer. Theoretically, radical chain reactions of unsaturated polyester resins (UPRs) yield homopolymers, but the addition of a reactive diluent, almost always styrene, leads to heterogeneous structures that can be attributed to successive molecular species arranged according to their mutual affinity. The reaction is initiated by an appropriate initiator (e.g., for UPRs) or by a hardener acting as a co-reactant (for epoxies, EPs).

The temperature increase required to start the reactions causes the system to accumulate heat, which adds to the heat of reaction (polymerizations are exothermic). Because polymers are poor thermal conductors, the resulting temperature rise can degrade the material and, in extreme cases, lead to spontaneous combustion of the resin.

The processability of the matrix is therefore related to its chemo-rheological state, which, through the degree of conversion and the temperature, determines the resin's flow properties. Under identical thermodynamic conditions, the rheology of the polymer derives primarily from its chemical nature, i.e., the average molecular stiffness and the intermolecular interaction forces. If the polymer's chemo-rheology does not meet the minimum conditions for processability, adding solvents can effectively modify its behavior by increasing molecular mobility and reducing intermolecular interactions; macroscopically, the main effect is a decrease in viscosity.

Generally, viscosity initially decreases with increasing temperature (Arrhenius-type behavior) but then rises abruptly once cross-linking begins. After a critical degree of conversion—the gel point—the system behaves like a gel: at this stage it is no longer possible to shape the material, and technological processability ends. Complete cross-linking takes longer because it is hindered by the low mobility of the high-molecular-weight oligomers that constitute the gel phase; however, the process must be considered finished only when polymerization is complete, since the gel, although un-processable, does not guarantee maintenance of the artifact's shape.

The final state of the material must therefore be a cross-linked glassy solid, achieved when the polymer's glass-transition temperature (which depends on the degree of polymerization) equals or exceeds the temperature of the reaction environment.

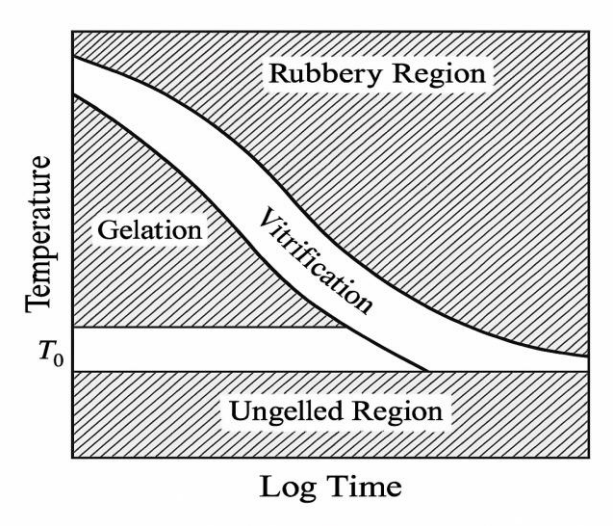

Figure 9- Temperature/time/transformation diagram for a thermosetting resin

Complete curing is achieved, if at constant temperature, in extremely long times so it is profitable to carry out a second

heating at higher temperatures; frequently, however, even after the second heating step, crosslinking is not completed for economic reasons.

The progress of the reaction, which terminates by competitive depletion of at least one of the species present, must therefore be analyzed in detail in order to be able to interact appropriately with the system to reduce its process time.

There are three intrinsic, non independent variables that describe the state of the resin during the progress of polymerization:

- temperature;
- viscosity;
- degree of conversion.

A complete model of crosslinking must therefore use these three parameters and must express a functional relationship between them; in addition, it is desirable that the analytical description be totally untethered from the reaction mechanism so as to fit perfectly with each type of thermosetting resin available (so far we spoke about the UPRs). The degree of reaction progress (or *degree of conversion*) can be associated with the heat of reaction (enthalpy type), which is an indirect measure of the number of chemical bonds that have formed:

$$\frac{\partial \alpha}{\partial t} = \frac{1}{H_{tot}} \frac{\partial H}{\partial t}$$

where the heat developed is closely related to the number of monomers (or oligomers) reacted for UPRs, to the average number of bonds formed in the case of EPs that proceed in stages through the formation of substituted amine compounds to a final ether.

The next step is to determine a relationship that expresses the degree of reaction as a function of time and temperature; Kamal (1974) proposed:

$$\frac{\partial \alpha}{\partial t} = (k_1 + k_2 \alpha^m)(1 - \alpha)^n$$

with m and n exponents to be determined experimentally and k_2 constant of a possible autocatalytic reaction (in EPs). An Arrhenius-type thermal dependence is assumed for k_i.

The reasoning carried out is correct as long as the control over the reaction is purely chemical; as soon as vitrification takes place, the reaction advances under *diffusive control*, so changes should be made to the model: this part will be explored in more detail later when process conditions dictate that control of the system should be protracted beyond the critical conversion at which, as seen, the forming of the material should be considered finished. For now we focus on the rheological aspect of the resin, the only one that directly influences the method and process times.

In agreement with Cox and Merz (1958), the elastic behavior of the polymer can be neglected when compared with viscous behavior. Viscosity is therefore the only parameter of interest and is considered to have the following temperature dependence:

$$\eta = Ae^{\frac{E_a}{RT}}$$

with the known meaning of the symbols. When, on the other hand, the elastic behavior is pronounced, that is, around the glass transition temperature, a more correct expression is given by Williams, Landel and Ferry:

$$ln\, a_T = ln\frac{\eta_{Tg}}{\eta} = \frac{C_1(T - Tg)}{C_2 + T - Tg}$$

The dependence on the degree of polymerization, however, is more complex and has been investigated at length. For linear polymers, an eq. of the type is considered valid:

$$\eta = const(Mr_G)^a$$

However, the model, developed for linear chains, provides acceptable results for cross-linked polymers as well. Combining the previous equations yields:

$$\frac{\eta(T,\alpha)}{\eta(T_r,0)} = \frac{\eta(T_r,\alpha)}{\eta(T_r,0)}\frac{\eta(T,\alpha)}{\eta(T_r,\alpha)} \Rightarrow \frac{\eta(T,\alpha)}{\eta(T_r,0)}$$
$$= \left(r_G\frac{M(\alpha)}{M_0}\right)^{3.4} \frac{exp(\,C_1(T_r - Tg(\alpha))/(C_2 + T_r - Tg(\alpha)))}{exp(\,C_1(T - Tg(\alpha))/(C_2 + T - Tg(\alpha)))}$$

in which T_r is the generic reference temperature.

Polymerization mechanisms

The traditional classification (Flory, 1953) distinguishes between *chain* and *step* reactions. The chain mechanism, in particular, includes radical and ionic polymerizations, the former of which is typical of UPR resins.

Stage reactions, on the other hand, include those by polycondensation and those by ring opening. Briefly reported are the kinetic patterns of polymerization starting with the radical:

$$initiator: R - O - O - R \rightarrow 2R - O\bullet$$

→ This is a high-value, wide-angle NASA review covering three decades of thermoplastic composites: maturity, performance, manufacturing routes, and fastener-less assembly/welding. Scan this QR code:

Prepregs

Pre-impregnated materials, universally shortened to *preprегs*, are semi-finished tapes or fabrics in which continuous or woven fibers are already saturated with a highly viscous, partially polymerized resin. Because most of the solvent or reaction heat has been removed during manufacture, the material can be stored at sub-zero or ambient temperatures and later consolidated in an autoclave, where simultaneous vacuum and external gas pressure produce aerospace laminates with porosity routinely below 1 %.

The reinforcement may be unidirectional carbon yarns or glass/aramid fabrics in plain, twill or multi-axial weaves, while the matrix can be a thermoset (epoxy, vinyl-ester) arrested in the so-called *B-stage* or a high-temperature thermoplastic such as polyimide. Thermoset prepregs arrive tacky at room temperature because the epoxy is only 15–25 % cured, a window that maximizes surface adhesion without locking the network—a property whose measurement is now standardized through probe-tack and peel methods adopted from ASTM practice.

By contrast, thermoplastic prepregs are fully polymerized and therefore dry and rigid; current R&D is exploring partially polymerized acrylic or other low-Tg binders to introduce room-temperature tack and drape without sacrificing melt strength during final consolidation.

During lay-up the prepreg plies are layered on the mould in orientations such as 0°, ±45° and 90°, debulked under vacuum, then cured in an autoclave for epoxies, or at higher temperatures and pressures when using PEEK, PEKK or PI matrices. The elevated pressure forces the liquid resin to

displace trapped air and wets the fiber bed completely, while the controlled heat cycle drives the thermoset to full conversion or melts/re-solidifies the thermoplastic.

Out-of-autoclave alternatives exist, but the autoclave route remains the benchmark for critical aerospace hardware thanks to its ability to combine high consolidation pressure with excellent temperature uniformity.

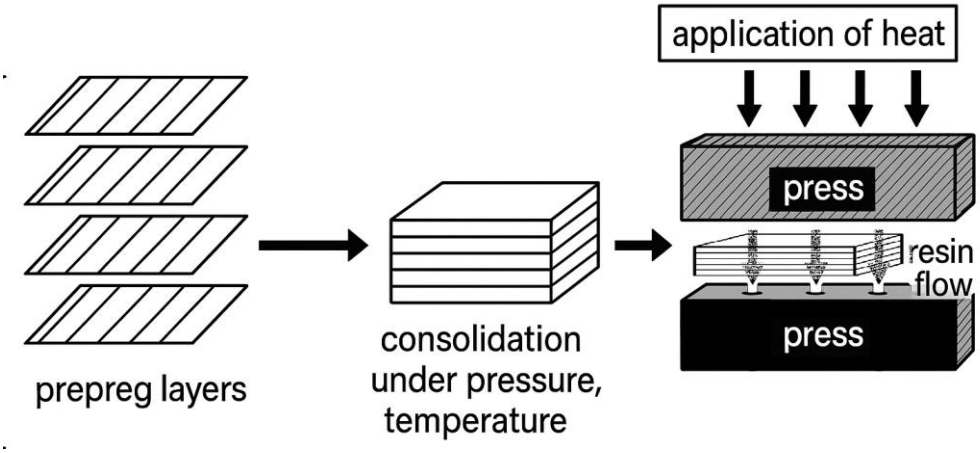

Figure 29 -General construction scheme of a laminate with prepreg overlay.

Solution-dip impregnation

Solution-Dip Impregnation (SDI) is widely regarded as the workhorse for producing solvent-based prepregs, because it combines gentle handling of the reinforcement with excellent matrix versatility.

In a single, unbroken pass, carbon, glass or aramid fiber, usually 12 k–24 k yarns or medium-weight woven fabrics, is paid off under a closed-loop tension of roughly 2–4 N per tow

and guided into a resin bath held at 30–50 °C. The bath contains 30–45 wt % solids, giving a manageable viscosity in the 0.3–0.9 Pa·s window; common solvents are acetone for unsaturated polyester, methyl-ethyl-ketone for high-Tg epoxies, and N-MP or DMAc when processing polyimide via its liquid polyamic-acid precursor.

Nip rollers loaded 5–15 kN m⁻¹ meter the coating, forcing resin deep into filament interstices and trimming the fiber-volume fraction to about 45–55 % for unidirectional tapes or 35–45 % for fabrics. The impregnated web then rises through a 4–6 m vertical oven where counter-flow air climbs from 90 °C at the entry to 180 °C at the exit. Within 60–120 s this gradient removes virtually all solvent (residual < 1 wt %) and, for thermosets, advances the resin to a tack-free B-stage with a glass-transition onset near 50 °C, ideal for storage yet readily re-activated during lay-up.

A twin set of chilled rollers brings the laminate temperature below 40 °C to prevent blocking; a thin LD-PE or PP release film is then laminated on, and the material is wound at line speeds of 5–20 m min⁻¹ (glass fabric can reach 30 m min⁻¹).

Modern SDI lines routinely deliver prepregs with void contents below 1 % and resin content accuracy better than ±1.5 wt %, while energy demand remains modest at roughly 0.4–0.6 kWh per square metre of product. Key engineering refinements include air knives set to 2 m s⁻¹ at the bath exit to avoid tow spreading, multi-zone ovens limited to ≤ 30 °C increments to suppress blistering, and closed-loop solvent recovery that captures more than 90 % of volatile emissions. Inline NIR sensors now track bath solids, allowing automatic solvent make-up and viscosity control, and wedge-slit coaters can replace open baths to cut solvent drag-out by around 40 %.

should ideally remain above 0.85, depending on the fiber areal weight, tow architecture, and resin viscosity. Process adjustments such as modulating the temperature profile, roller gap, or pulling speed are used to maintain H within an acceptable range.

The autoclave process

The autoclave curing process for composite materials dates to 1954 and has since established itself as the benchmark method for the fabrication of high-performance laminates. Its widespread use is historically rooted in the aerospace and defense sectors, where structural integrity, weight reduction, and reliability are paramount. Over the decades, the technology has been selectively adopted in aviation, motorsport, premium automotive production, competitive marine applications, and advanced sports equipment, wherever precision and mechanical consistency outweigh processing costs.

Autoclave processing is centered on the consolidation and polymerization of fiber-reinforced prepregs (typically thermosetting systems) under controlled heat and pressure. The laminate stack is vacuum bagged and placed within a pressure vessel, where it is subjected to a calibrated temperature and pressure cycle. The elevated pressure, usually in the range of 6 to 7 bar, enhances fiber-resin wet-out, promotes gas evacuation, and suppresses the formation of voids or dry spots during cure. The temperature, meanwhile, activates the curing kinetics of the resin, guiding it from a low-viscosity liquid state to a crosslinked solid.

Despite the solid theoretical foundations of the process (including reaction kinetics, heat transfer equations, and resin rheology models) the practical implementation remains complex due to the large number of interdependent variables. Parameters such as *temperature ramp rates, dwell times, applied pressure, vacuum quality, resin viscosity, tool thermal inertia, part thickness, and fiber architecture* all interact, often non-linearly. As a result, process optimization tends to rely not

only on predictive simulations but also on *empirical calibration,* supported by experimental trials to fine-tune the cycle for each specific laminate geometry and resin system.

A key performance advantage of autoclave curing lies in its ability to minimize void content. Under properly controlled conditions, final void contents are typically maintained below 1%, compared to the 2%–4% often observed in oven-cured or out-of-autoclave (OOA) composites. This substantial reduction in porosity translates into significant gains in mechanical performance, especially in terms of interlaminar shear strength, fatigue resistance, and compression after impact. These properties are critical in load-bearing aerospace structures, where internal defects act as stress concentrators and limit fatigue life.

Void minimization is achieved by exploiting the pressure gradient established during the cure. As the matrix transitions from a low-viscosity to a gelled state, the applied pressure forces the resin to flow through the inter-fiber voids in a direction orthogonal to the laminate plane. This flow carries along trapped air, volatiles, and microbubbles that may originate from lay-up defects or from chemical byproducts during crosslinking. These gases are expelled via breather and vent paths, aided by the vacuum applied inside the bag.

To enable effective flow and void purging, the starting prepreg system must contain more resin than what will remain in the final cured composite. Typically, aerospace-grade prepregs have an initial resin content of around 35%–42% by weight, which corresponds to approximately 50%–55% by volume, depending on fiber type and architecture. During cure, part of this resin bleeds out or fills minor tool gaps, resulting in a final matrix fraction closer to the desired 30%–35% by volume. This

excess ensures full wet-out and gap filling without risking resin starvation.

The combination of external pressure, precise thermal control, and a sacrificial resin surplus yields composite parts with exceptional surface finish, dimensional stability, and mechanical uniformity. Although autoclave processing is capital-intensive and requires rigorous control of process parameters, its unmatched quality and repeatability make it indispensable for certified aerospace structures, critical defense applications, and experimental platforms where reliability is non-negotiable. Its legacy, refined over nearly seven decades, continues to define the *highest standard* in composite material fabrication.

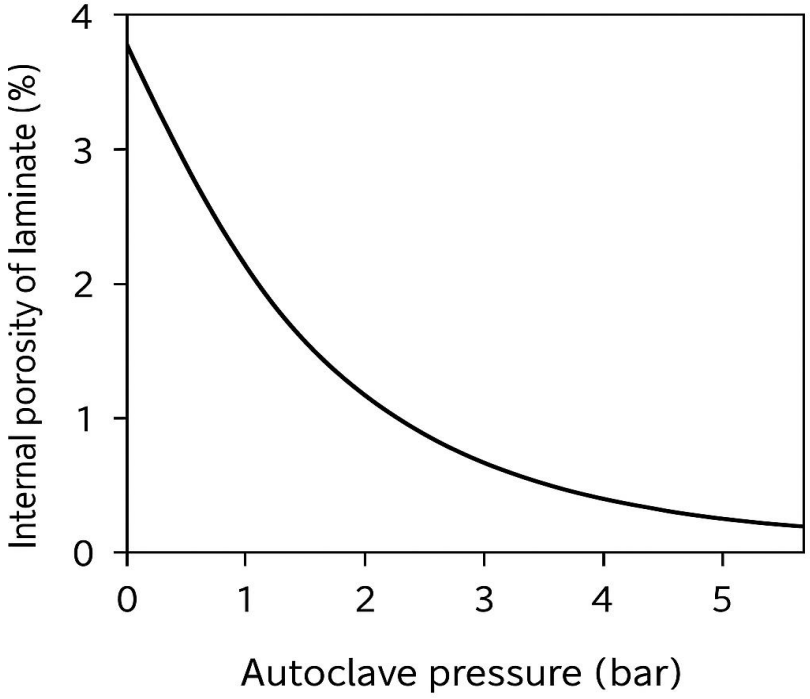

Figure 54 - Plot of the composites internal porosity vs autoclave pressure

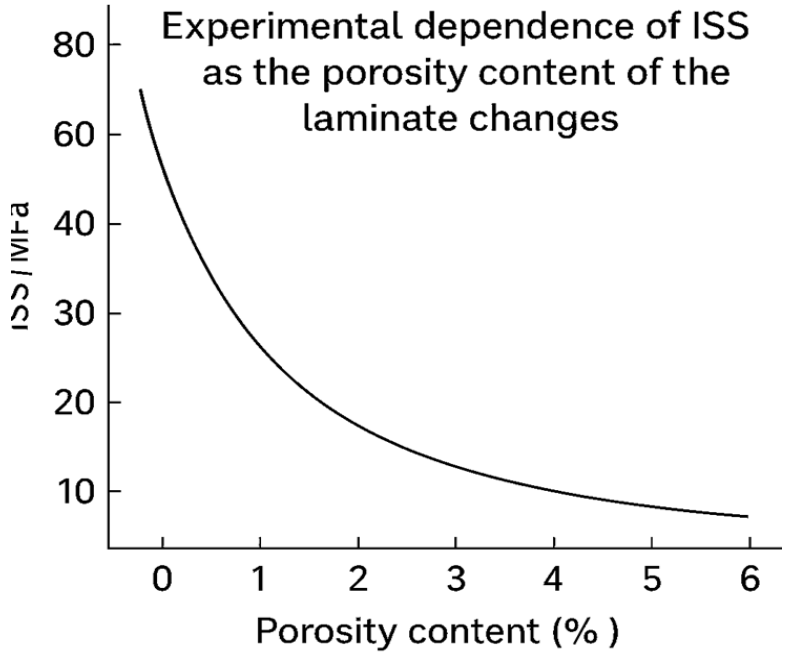

Figure 55 - Plot of the Interlaminar Shear Strength (ISS) vs porosity content in the laminate (experimental data)

Porosity in composite laminates originates primarily from two sources: gases and vapors entrapped during lay-up, such as air and moisture incorporated into the resin system, and solvent vapors, which often exert a vapor pressure higher than the internal pressure of the autoclave during cure. Both phenomena, if not properly controlled, contribute to void formation and compromise the structural integrity of the final part.

Resin flow control plays a critical role in minimizing porosity and is typically managed by adjusting external pressure at strategic points in the thermal cycle. In thermosetting systems, pressure is increased as soon as the resin begins to chemically polymerize and viscosity rises. This intervention avoids uncontrolled flow and prevents premature resin stiffening that

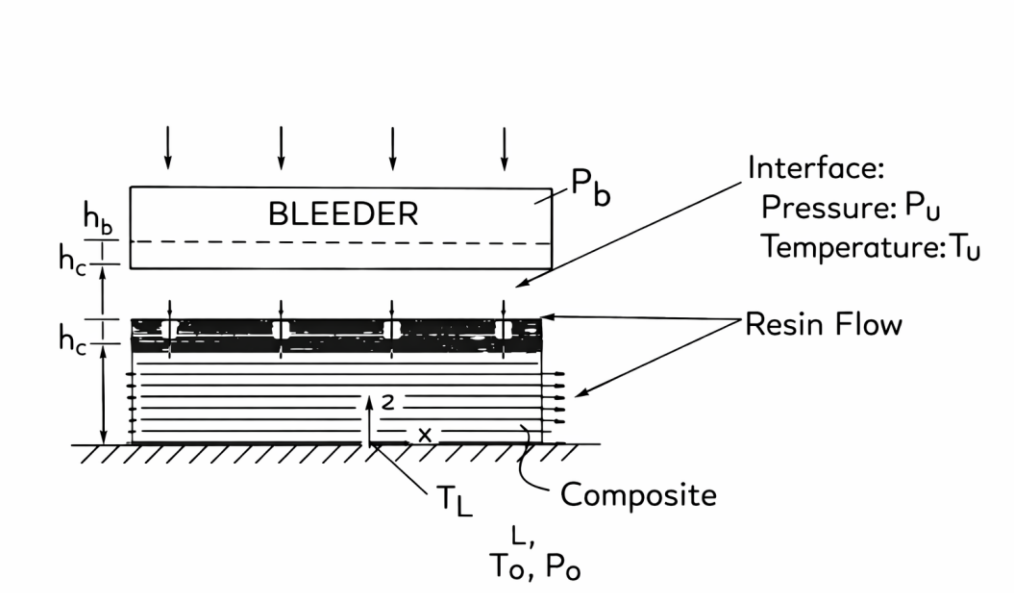

Figure 65 - Fluid dynamic model parameters

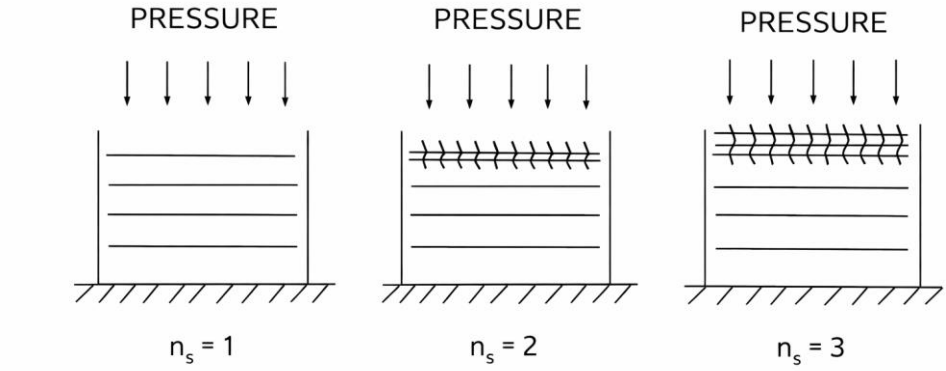

Figure 66 - Sequential compaction of plies

The resin flow in the direction of the bleeder is given by a simple mass flow continuity equation:

$$\dot{m} = \rho_r A(z)\dot{z}(z)$$

From Darcy's Law:

$$\dot{z} = \frac{S}{\mu}\frac{dp}{dz}$$

Substituting the velocity into the previous equation gives:

$$\dot{m} = \rho_r A(z)\dot{z}(z) = \rho_r A(z)\frac{S}{\int_0^{hc}\mu dz}(p_C - p_U)$$

having denoted by h_C the instantaneous thickness of the compacted layers through which the resin flows. The quantities with subscript C refer to the position with elevation h_C; p_u is the pressure at the bleeder/composite interface. Obviously, continuity conditions dictate that a similar equation can be written for the first layers of the bleeder in contact with the laminate:

$$\dot{m} = \rho_r A(z)\dot{z}(z) = \rho_r A(z)\dot{z}_b(z)$$

$$\dot{m} = \rho_r A(z)\dot{z}(z) = \rho_r A(z)\frac{S_b}{\mu}\frac{p_U - p_b}{hb}$$

Bartlett, Loos and Springer proposed the following alternative expression:

$$\dot{m} = \frac{\partial m}{\partial t} = \frac{\rho_r A S_C}{\int_0^{hc}\mu dz}\left(\frac{p_0 - p_b}{1 + G(t)}\right)$$

$$G(t) = \frac{S_C}{S_b}\frac{\mu_b hb}{\int_0^{hc}\mu dz}$$

$G(t)$ is a correction factor that converges numerical results don experimental results.

The mass of polymer leaving the laminate at time t is obtained by simple integration:

$$m = \int_0^t \frac{\partial m}{\partial t} dt$$

while the thickness of the bleeder affected by the resin flow results (V_b) represents the porosity of the bleeder):

$$hb = \frac{1}{\rho_r V_b A} \int_0^t \frac{\partial m}{\partial t} dt$$

Diffusive model

As previously noted, the presence of voids within composite laminates is primarily attributed to entrapped air and moisture introduced during the lay-up process. The diffusive model, originally developed by Spring, Loos, and Kardos, provides a framework for understanding the evolution of these inclusions during curing. According to the model, voids are assumed to be perfectly spherical gas inclusions, whose size and pressure vary dynamically in response to changing thermal and pressure conditions applied to the composite.

In addition to mechanical compression and thermal expansion effects, the model incorporates diffusive transport mechanisms, particularly the migration of water vapor molecules into existing voids. This process, known as *core accretion*, causes the inclusions to grow in volume as water diffuses from the surrounding resin matrix into the gas phase within the bubble. The resulting behavior depends on cure temperature, ambient pressure, resin permeability, and the

partial pressure of water vapor, all of which contribute to the final void size, distribution, and stability within the laminate.

This model highlights the importance of both initial lay-up quality and thermal-pressure control during curing, as even small amounts of trapped moisture can evolve into significant porosity if not properly managed through process design or material selection.

The size of the voids is thus related to the acting pressure and surface tension of the polymer during curing:

$$p_{in} - p_{out} = \frac{4\sigma}{d}$$

The internal pressure, then, is sum of the partial pressures of air and vapor:

$$p_{in} = pp_{air} + pp_{vapor}$$

each a function of the temperature, mass and volume available to the two species.

The pressure acting on the inclusion is known from the fluid-dynamic model, the temperature from the thermochemical model; known that it is the mass, it is then possible to trace the average diameter of the voids.

We will now then go on to calculate a time-dependent function of the mass of such inclusions, which, according to the assumptions made, increases by diffusive mechanism. From Fick's 2nd law, calling c the vapor concentration and D the diffusivity:

$$\frac{\partial c}{\partial t} = D\left(\frac{\partial^2 C}{\partial r^2} + \frac{2}{r}\frac{\partial c}{\partial r}\right)$$

Therefore, while micromechanical models often assume ideal conditions, real-world evaluations must take into account the inevitable influence of void content on stiffness, strength, fatigue resistance, and environmental durability. Defining V_v the ratio of the volume of voids to the theoretical volume of the composite, we have:

$$V_v = \frac{v_v}{v_c} = \frac{v_{ce} - v_{ct}}{v_{ce}} = \frac{w_c/\rho_{ce} - w_c/\rho_{ct}}{w_c/\rho_{ce}} = \frac{\rho_{ct} - \rho_{ce}}{\rho_{ct}}$$

With obvious meaning of the symbols.

The percentage of voids can then be calculated from the knowledge of the actual density and theoretical density.

Longitudinal elastic properties

With reference to the figure below, when a tensile load P_C is applied longitudinally to a unidirectional composite lamina, the overall response of the material results from the combined effect of the two constituent phases: the reinforcing fibers and the polymer matrix. From a basic equilibrium standpoint, the total load applied to the composite is distributed between the fibers (which carry load Pf) and the matrix (which carries load Pm).

Because both constituents are bonded and deform together in the longitudinal direction, they experience the same axial strain. This fundamental assumption of equal strain in the fiber and matrix under longitudinal loading enables the derivation of the composite's effective Young's modulus in the fiber direction, often denoted as $E1$. In this configuration, the fibers, being significantly stiffer, contribute the majority of the stiffness, while the matrix primarily plays a supporting role in transferring stress and maintaining the integrity of the material system.

The overall stiffness of the lamina in the longitudinal direction is, therefore, a function of the stiffness of each phase and their respective volume fractions. An increased proportion of fibers typically results in a marked improvement in the axial modulus and strength of the composite. However, there is a practical limit to fiber content beyond which processing becomes difficult and mechanical performance may degrade due to insufficient matrix to properly wet and bind the fibers.

In engineering practice, the effective longitudinal modulus can be estimated with reasonable accuracy using micromechanical models that assume perfect bonding and uniform strain

distribution. This allows the designer to predict the performance of the lamina based on the known properties of its constituents and tailor the reinforcement ratio accordingly for the intended application.

It is worth noting that this model assumes continuous, aligned fibers and no defects or voids in the microstructure. In real-world composites, slight deviations from perfect alignment, fiber waviness, and void content may reduce the actual stiffness compared to the idealized predictions.

The result is that the longitudinal properties of a unidirectional composite (such as stiffness, strength, and load-carrying capability) are primarily governed by the fiber characteristics and their alignment, making fiber selection and volume control critical in high-performance applications.

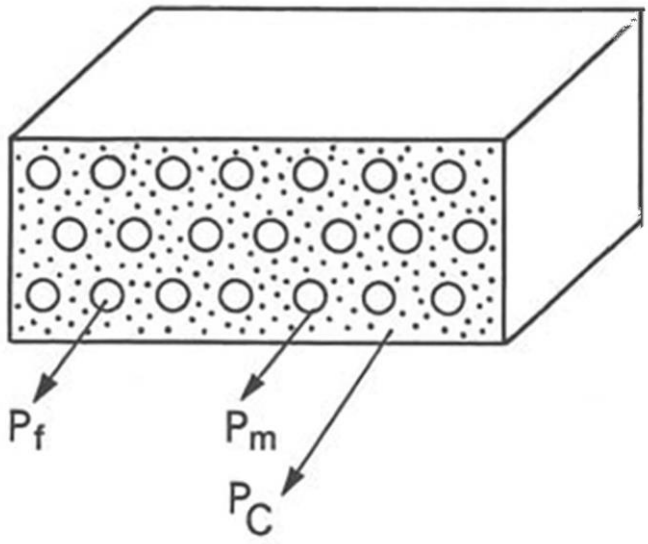

Figure 122 - Loads on fiber, matrix and global (on composite)

$$P_c = P_f + P_m$$

Which, in terms of tensions, results:

$$\sigma_c A = \sigma_f A_f + \sigma_m A_m$$

with obvious meaning of the symbols. Dividing by the cross-sectional area and taking into account that for the assumptions made the ratio of the areas coincides with the volume fractions, we have:

$$\sigma_c = \sigma_f V_f + \sigma_m V_m$$

This formula shows that the stresses between matrix and fiber are distributed proportionally to their respective volume fractions: for this reason, in many cases of practical interest, only the fiber contribution is considered. Under the usual assumption of perfect fiber-matrix adhesion, i.e., in the absence of relative sliding, we also have that the fiber strain ε_f coincides with that of the matrix ε_m and thus of the composite ε_c i.e:

$$\varepsilon_f = \varepsilon_m = \varepsilon_c = \varepsilon$$

We then arrive at the expression:

$$\frac{d\sigma_c}{d\varepsilon} = \frac{d\sigma_f}{d\varepsilon} V_f + \frac{d\sigma_m}{d\varepsilon} V_m$$

Under the assumption that matrix and fiber have linear elastic behavior:

$$E_c = E_f V_f + E_m V_m$$

This equation is remembered as *the rule of mixtures* (R.O.M.) and was derived in the case where the two phases exhibit strictly linear elastic proportional behavior: a similar formulation, it will be recalled, applies to density and stresses.

The *rules of mixtures* are foundational principles in composite micromechanics that allow engineers to estimate the effective properties of a lamina based on the properties of its individual components, typically the fiber and the matrix. These rules are particularly useful in predicting elastic moduli, strengths, and other mechanical attributes under the assumption of ideal bonding and uniform stress or strain distribution.

In their simplest form, the rules of mixtures provide upper and lower bounds for material behavior. For instance, when dealing with unidirectional composites under loading parallel to the fibers, the longitudinal modulus is typically calculated as a linear combination of the fiber and matrix moduli weighted by their respective volume fractions. This results in a value that lies between the individual moduli, reflecting a smooth transition in behavior from one material phase to the other.

However, when one of the constituents, most often the matrix, exhibits nonlinear behavior (e.g., plasticity, viscoelasticity, or damage), the laminate's response also begins to deviate from the ideal linear predictions, although the deviation is usually moderated by the stiffer and more linear behavior of the reinforcing fibers. In such cases, the overall behavior of the lamina becomes a complex interplay between the nonlinear effects of the matrix and the constraining influence of the fibers. As a result, while the rule of mixtures still offers a useful approximation, more advanced micromechanical models are often required to accurately predict the stress-strain response and failure mechanisms under real-world loading conditions.

Ultimately, the effectiveness of the rule of mixtures depends on the fiber distribution, orientation, bonding quality, and strain compatibility between phases, factors that need to be accounted for when transitioning from idealized theory to practical application.

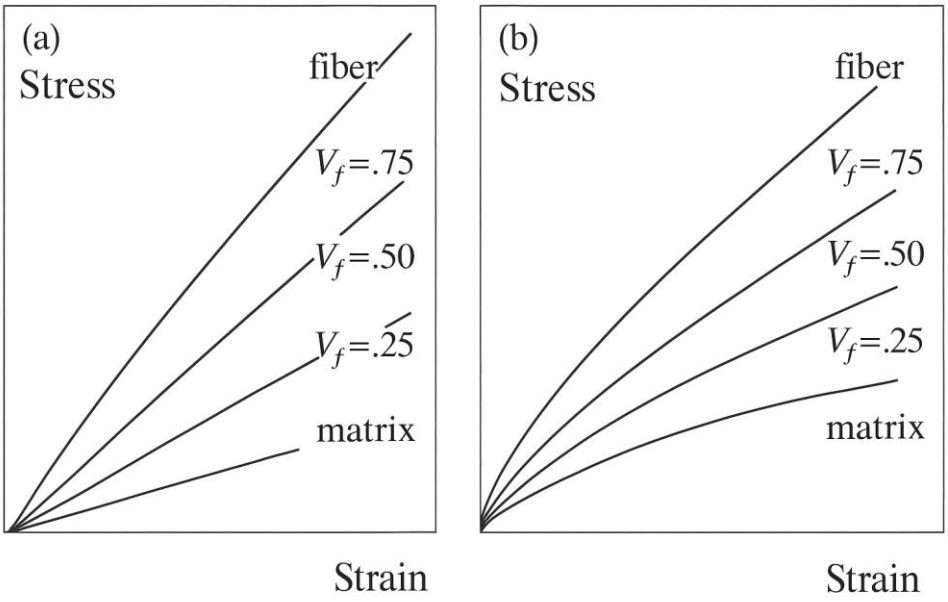

Figure 123 - Rule of mixtures on the stress/strain diagram for different fiber volume ratios. On the left there is a matrix with brittle behavior, on the right a more ductile one

In composite laminates subjected to tensile loading, particularly those with high fiber volume fractions or with fibers possessing a modulus of elasticity significantly higher than that of the matrix, the mechanical behavior of the composite closely mirrors that of the fiber. This is due to the fact that the fibers, being stiffer, sustain the majority of the load. As a result, the characteristic stress–strain (σ–ε) response of the composite is nearly linear and follows the behavior of the fiber up to failure, which is typically brittle.

On the other hand, the polymeric matrix often exhibits non-linear behavior beyond low strain levels, typically viscoelastic or plastic depending on the temperature and strain rate. However, in highly fiber-dominated laminates, this matrix

nonlinearity contributes only marginally to the overall response and is commonly neglected in modeling, assuming instead that the laminate behaves as a linear elastic material.

From a mechanical point of view, when a uniaxial tensile force is applied, the strain in the fiber and matrix must remain equal because they are bound together: this is a fundamental assumption in micromechanics. Given this constraint, and by applying Hooke's law to each phase, one can analyze how the load partitions between the fiber and the matrix. Since strain is shared, the stress carried by each phase is proportional to its modulus of elasticity and volume fraction. This partitioning reveals that, for high-stiffness and high-volume fiber content, the fiber bears the majority of the mechanical load, which underscores its dominant role in defining the composite's strength and stiffness.

$$\frac{\sigma_f}{E_f} = \frac{\sigma_m}{E_m} \Rightarrow \frac{\sigma_f A_f}{E_f} A_m = \frac{\sigma_m A_m}{E_m} A_f \Rightarrow \frac{P_f}{P_m} = \frac{E_f}{E_m} \frac{V_f}{V_m}$$

Interestingly, the ratio of the load carried by the fiber to that carried by the matrix in a composite follows a linear relationship based on the relative values of their Young’s moduli and their respective volume fractions. This means that, once the fiber and matrix volume fractions are established, the efficiency with which the fiber’s superior mechanical properties are exploited depends directly on the stiffness contrast between the two phases. To maximize the benefits of using high-strength fibers, it is therefore essential that the fiber’s Young’s modulus be significantly higher than that of the surrounding matrix.

In practical applications, such as with carbon fiber-reinforced composites, this condition is readily met: the Young’s modulus of carbon fibers is typically more than 60 times greater than

that of the polymer matrix. As a result, even with moderate fiber volume fractions, more than 90 percent of the tensile load is generally supported by the fibers. This highlights the dominant structural role played by the reinforcement.

While technically feasible to manufacture composites with fiber volume fractions approaching 90 percent, such concentrations are rarely used. Most high-performance composites are produced with fiber contents below 80 percent. This is because exceeding that threshold can lead to diminished mechanical performance due to processing issues, specifically, difficulties in achieving uniform wetting and adhesion between fibers and matrix. Poor wetting can result in weak interfacial bonding, which becomes a limiting factor in the material's ability to transfer stresses effectively. Moreover, the achievable volume fraction is strongly influenced by the specific manufacturing technique employed, with methods like resin transfer molding (RTM), prepreg layup, or filament winding each having practical upper limits defined by flow characteristics and fiber packing behavior.

As for the elastic modulus in shear, denoted G_{12}, it corresponds to the ratio between the tangential stress applied to the lamina in its mid-plane and the angular deformation that this stress induces. In other words, when the lamina is subjected to an in-plane shear load, the resistance it offers to this deformation is governed by the shear modulus. It is important to note that, unlike the longitudinal modulus E_1, which is largely influenced by the stiffness of the fibers, the shear modulus is primarily affected by the matrix properties and the interaction between fibers and matrix. This is because, under shear loading, it is the matrix that accommodates most of the deformation between the adjacent fibers, transmitting the load from one fiber to another.

In composites where the matrix is relatively soft and the fiber content is high, G_{12} can assume relatively low values despite the high overall stiffness in the longitudinal direction. This behavior reflects the anisotropic nature of the composite, where performance varies markedly depending on the direction of loading.

Poisson's coefficient ν_{12}, on the other hand, measures the tendency of the material to contract in the transverse direction (direction 2) when stretched in the longitudinal direction (direction 1). It is defined as the ratio between the transverse strain and the axial strain under a uniaxial tensile stress in the direction of the fibers. Although this parameter is dimensionless, it plays a significant role in characterizing the elastic response of the lamina, especially in applications involving multi-axial stress states or thermal expansions.

To better understand these properties, imagine a rectangular lamina composed of unidirectional fibers embedded in a polymer matrix. When the laminate is pulled along the fiber direction, the fibers carry the majority of the load and deform very little. The matrix, comparatively more compliant, is pulled along with the fibers and contracts slightly in the transverse direction. This transverse contraction defines ν_{12}.

If, instead, a shear load is applied (attempting to slide the upper face of the lamina relative to the lower one) it is again the matrix that responds predominantly to this deformation, as the fibers offer little resistance to such shearing motion. As a result, the value of G_{12} depends significantly on the matrix modulus and the extent to which the fibers restrict shear strains via mechanical interlocking and adhesion.

These parameters, although not as immediately intuitive as tensile strength or Young’s modulus, are essential to

accurately modeling the response of composite laminates under service conditions, particularly when dealing with complex loadings, vibration, or fatigue.

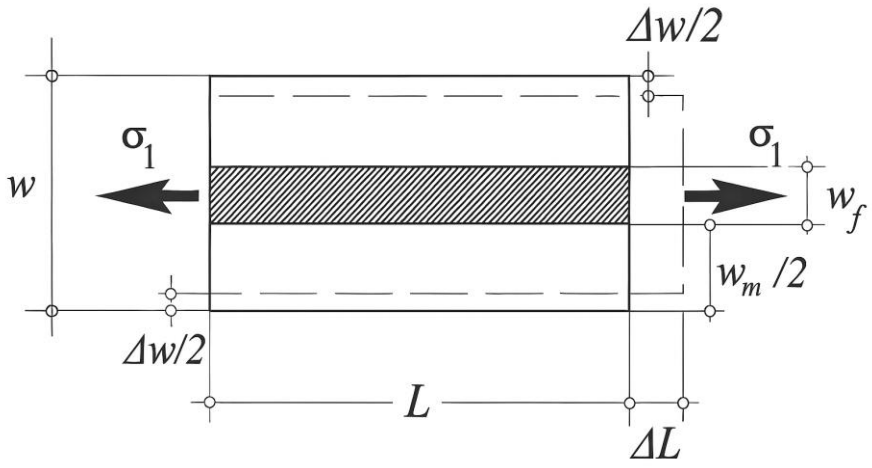

Figure 124 - Representative elemental volume

With reference to the notation shown in the figure, any longitudinal tension induces a transverse strain in the lamina equal to:

$$\varepsilon_2 = \frac{\Delta w}{w} = \frac{\Delta w_f + \Delta w_m}{w} = \frac{-\nu_f \varepsilon_1 w_f - \nu_m \varepsilon_1 w_m}{w}$$

Noting that the ratio (w_i/w) coincides for the case seen with the relative volume concentration, we have:

$$\nu_{12} = -\frac{\varepsilon_2}{\varepsilon_1} = \nu_f V_f + \nu_m V_m$$

This relationship demonstrates that, much like the longitudinal modulus of elasticity, the Poisson's ratio of a composite material can be approximated using the familiar rule of mixtures applied to the fiber and matrix components. In practice, this equation is frequently used in reverse, that is, to estimate the Poisson's ratio of the fiber phase, which is often

Composites exhibit significantly higher specific strength (50–150%) and stiffness (40–120%) compared to traditional materials such as metals, ceramics, and polymers.

- **Weight Reduction Capability:**

Potential weight savings in engineered components range from approximately 20% to 60%, making composites highly beneficial in weight-critical sectors like aerospace and automotive.

- **Enhanced Thermal Stability:**

Composites effectively operate within elevated temperature ranges (approximately 120°C to 300°C), clearly outperforming typical polymeric materials.

Overview of composites material classes

This overview chapter presents class-level trade-off charts for key composite material families.

This high-level view of the composite materials landscape is useful before delving into the detailed properties in the following sections.

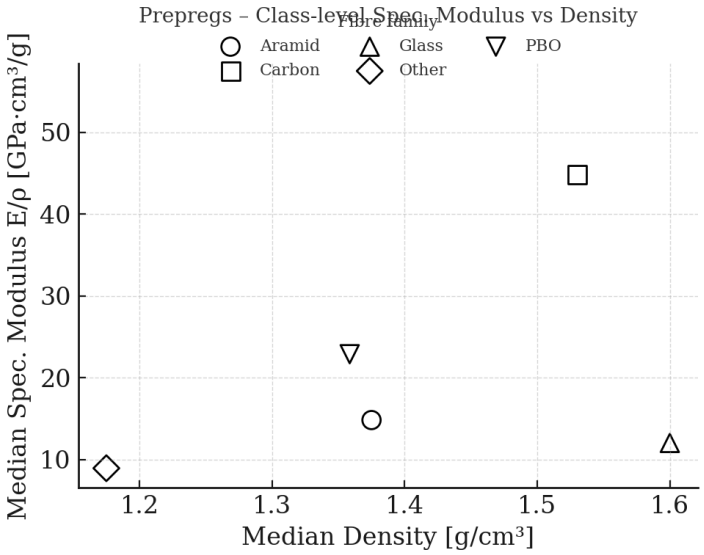

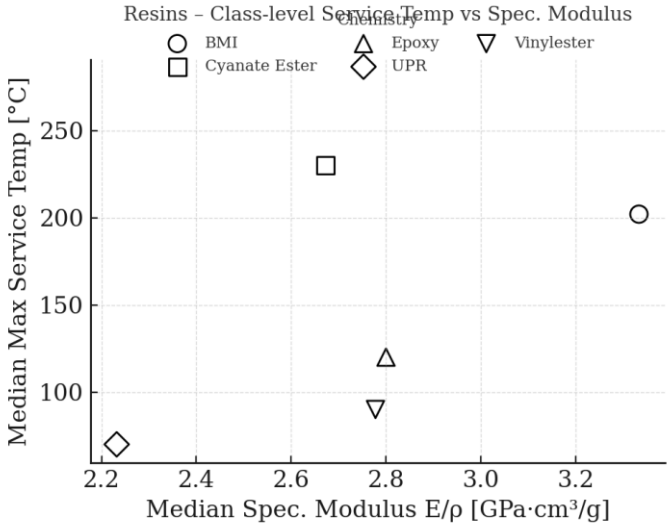

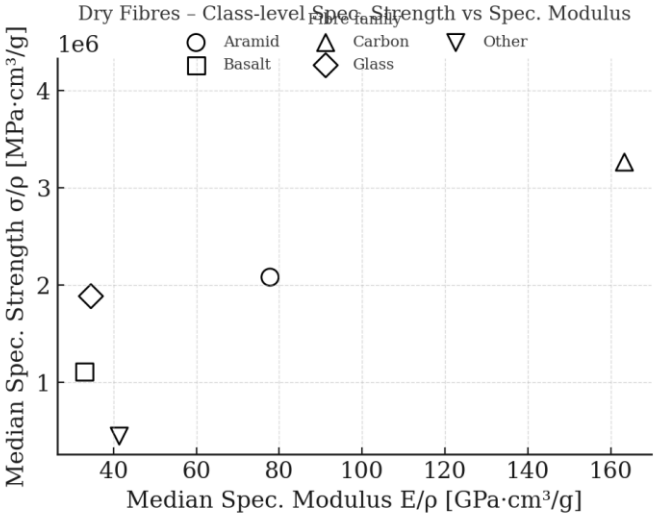
Dry Fibres – Class-level Spec. Strength vs Spec. Modulus
Fibre family
Aramid
Carbon
Other
Basalt
Glass
1e6
Median Spec. Strength σ/ρ [MPa·cm³/g]
Median Spec. Modulus E/ρ [GPa·cm³/g]

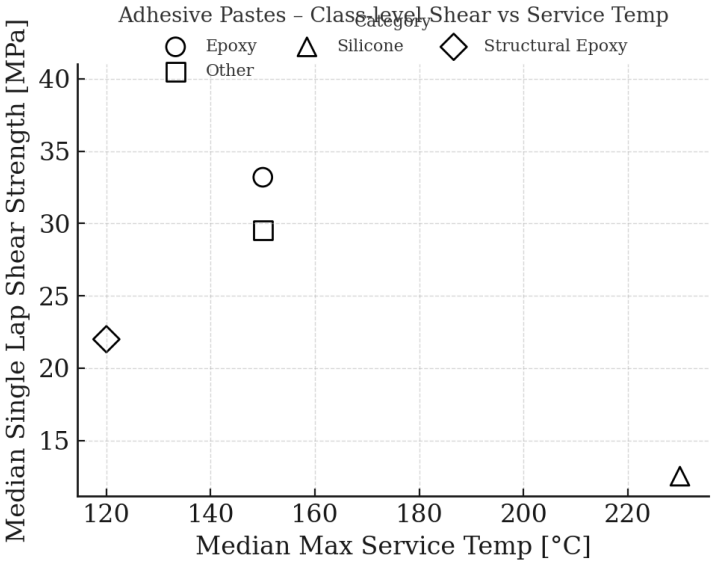
Adhesive Pastes – Class-level Shear vs Service Temp
Category
Epoxy
Silicone
Structural Epoxy
Other
Median Single Lap Shear Strength [MPa]
Median Max Service Temp [°C]

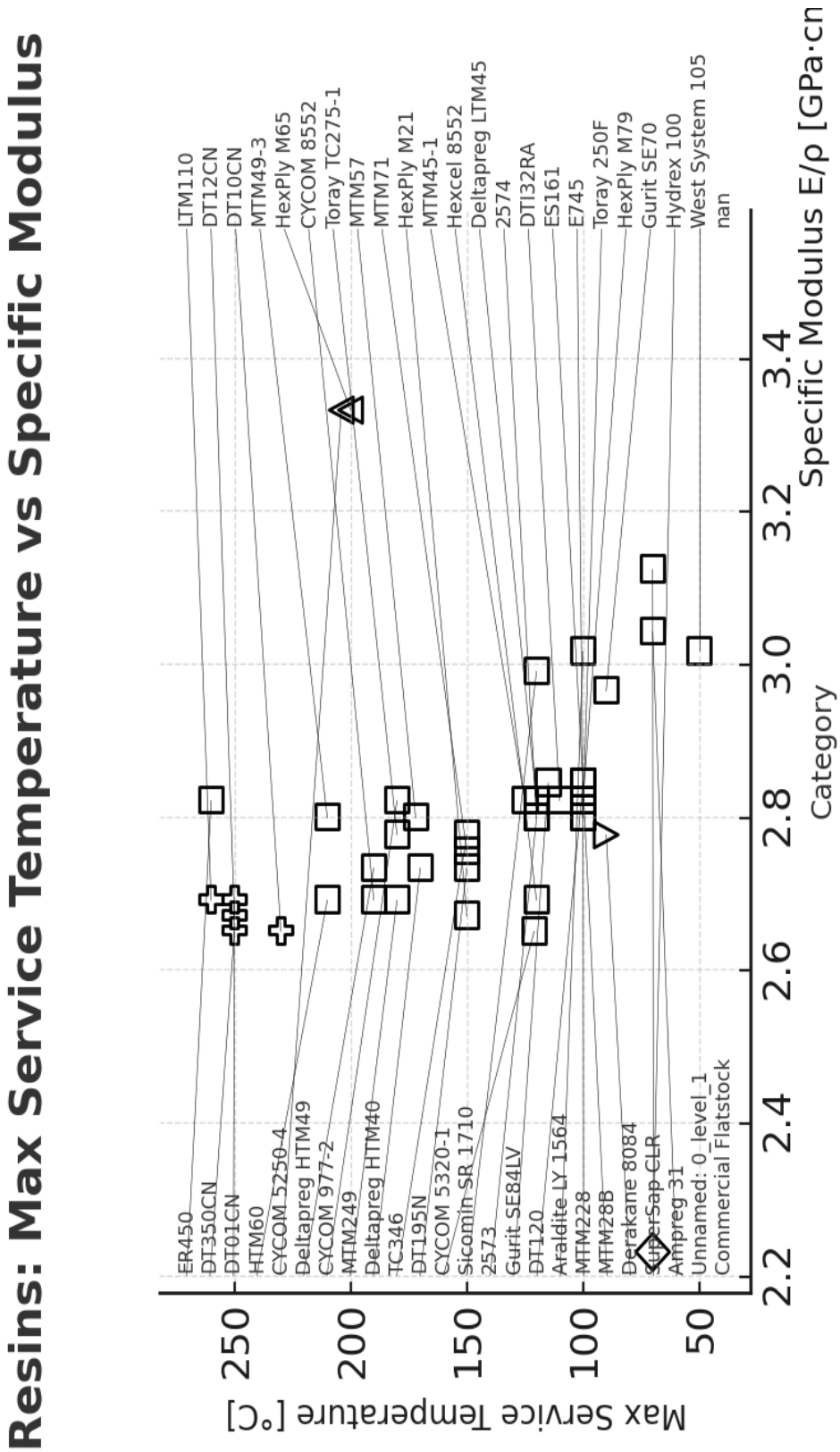
Resins: Max Service Temperature vs Specific Modulus
Max Service Temperature [°C]
Specific Modulus E/ρ [GPa·cn
Category
Other
Epoxy
BMI
UPR
Vinylester
Cyanate Ester
LTM110
DT12CN
DT10CN
MTM49-3
HexPly M65
CYCOM 8552
Toray TC275-1
MTM57
MTM71
HexPly M21
MTM45-1
Hexcel 8552
Deltapreg LTM45
2574
DTI32RA
ES161
E745
Toray 250F
HexPly M79
Gurit SE70
Hydrex 100
West System 105
nan
ER450
DT350CN
DT01CN
HIM60
CYCOM 5250-4
Deltapreg HTM49
CYCOM 977-2
MTM249
Deltapreg HTM40
TC346
DT195N
CYCOM 5320-1
Sicomin SR 1710
2573
Gurit SE84LV
DT120
Araldite LY 1564
MTM228
MTM28B
Derakane 8084
SuperSap CLR
Ampreg 31
Unnamed: 0_level_1
Commercial Flatstock

Adhesive Pastes: Density vs Max Service Temperature

Adhesive paste density vs max service temperature reveals thermal limits of bonding materials, important for assemblies exposed to specific temperature ranges.

High-temperature silicones can withstand 300 °C at densities ~1.1 g/cm³, but their specific strength remains low (<0.3 GPa·cm³/g), important for non-structural bonding.